

Virtual inertia grid control with LED lamp driver

Eberhard Waffenschmidt

CIRE (Cologne Institute for Renewable Energy) at
TH-Köln (Cologne University of Applied Sciences)
Betzdorferstraße 2, 50679 Cologne, Germany
eberhard.waffenschmidt@th-koeln.de

Abstract— Soon, rotating inertia of generators use for grid control must be replaced due to the growth of distributed renewable energies. Here, we propose to let also electronic loads contribute to future virtual inertia. It is suggested to use DC link capacitors of power supplies for this task. This requires 5 W, 50 J and a capacitor size of about 200 cm³ per installed kW, corresponding to the size of single phase DC link capacitors. It is shown that the additional power ripple (and thus current ripple) is in the order of 0.1% and the voltage ripple of the intermediate voltage will typically remain between +/-3.6%. The related control can be easily extended by adding a voltage signal to the control voltage, which is proportional to the frequency deviation. Then, the existing power factor correction controller inherently sets the required additional power fluctuation required for the virtual inertia function.

1 INTRODUCTION

Renewable energy sources put new burdens on the electrical power grid. While fluctuating generation can be compensated by storages [1], the grid control also faces challenges: At certain times, renewable energy sources contribute already up to 85% to the power consumption in Germany [2], and soon shares of 100% for longer periods are expected [3].

Most of this power is generated by electronic power converters without rotating inertia. Fortunately, Germany's grid is part of the ENTSO-E, European Network of Transmission System Operators for Electricity, and today the missing inertia can be compensated by the other members, which have less renewable energies [4]. However, in future, also their inertia may vanish leading to larger frequency deviations.

Then this instantaneous reaction on load steps must be covered by electronic inverters [6] [7] [8]. To provide instantaneous reaction control, [4] mentions the following solutions: batteries combined with photovoltaic (PV) systems or curbing the generation in order to have a margin for positive control power. Both solutions are costly. Another possibility is using the inertia of wind rotors, like offered by several wind generator manufactures and which is required in Quebec's (Canda) according to its grid code [9]. However, any change of the rotating inertia leads to a deviation from the maximum power point of the wind turbine, and a certain time is necessary for the wind turbine to recover from the deviation [10]. This leads to some financial losses. Finally, modifying no longer used rotating generators as control power devices are possible. However, these

solutions are either costly or not sufficient. In its latest grid code ENTSO-E requires synthetic inertia for type C power park modules of more than one MW in the case of a low frequency event, but not during normal operation (article 16.2 and 49.5 [11]).

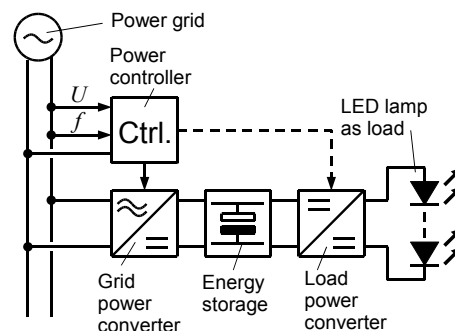


Figure 1: Considered topology.

In [12] DC link capacitors of PV inverters are used for virtual inertia. Here, it is proposed to let also electronic loads contribute to future virtual inertia. It is suggested to use DC link capacitors of power supplies for this task. As an example for a load, an electronic driver for a light emitting diode (LED) is selected. Figure 1 shows the considered topology, which is nothing special related to its hardware. This publication investigates, whether such devices can give a sufficient contribution (chapter 2 and 3) and how they are stressed by the additional functionality (chapter 4), which is similar to [12] in large parts. Then it is shown how to integrate a related control to existing hardware (chapter 5) and first measurements are presented (chapter 6).

2 POWER AND ENERGY REQUIREMENTS

In a first step, the requirements for the worst case in the European ENTSO-E grid are derived. It is assumed that only the instantaneous reaction is considered, while the following primary control is taken over by dedicated sources in the grid. To get the power and energy requirements, the methodology and data of reference [4] is used (see Figure 2): a worst case event of a sudden lack of 3 GW power in the ENTSO-E grid is assumed. This requires 372 MW in the German grid. Assuming the primary control taking over with a linear increase within 20 s [4], this requires energy of 3720 MJ. This power and energy is related to an assumed installed power of loads of 80 GW in Germany. Taking this 80 GW as a reference leads to 4.6 W/kW, rounded up to 5 W/kW. Concluding,

additional power of 5 W and energy of 50 J per installed kW power capacity is needed to cover one worst case event. It should be noted that these numbers refer to the installed power of the systems, not to the power they actually consume. Thus, the power of one converter needed for the virtual inertia is related to the rated power and not to the power it actually consumes.

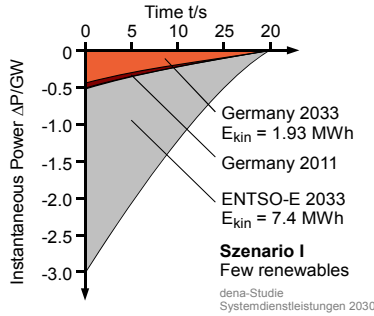


Figure 2: Power requirements for a worst case load step of 3 GW in the European ENTSO-E grid [3].

This level of power can easily be processed by the first stage of the power supply. The amount of energy relates to the energy content of a somewhat larger DC link capacitor (details see following chapter).

3 NEEDED CAPACITOR SIZE

Typically, the size of a capacitor relates to its maximum energy content. To determine the interdependence, the capacity, rated voltage, diameter and height of more than 200 electrolytic capacitors are collected from the website of an electronic components distributor [13]. Rated energy and volume are calculated from this data and shown in Figure 3. In real circuits, not the maximum rated energy capability E_{max} can be used, because the capacitor is discharged from the maximum voltage U_{max} only by a voltage difference ΔU . Then the usable energy E_{use} is:

(1)

$$E_{use} = E_{max} \cdot [1 - (1 - \Delta U / U_{max})^2]$$

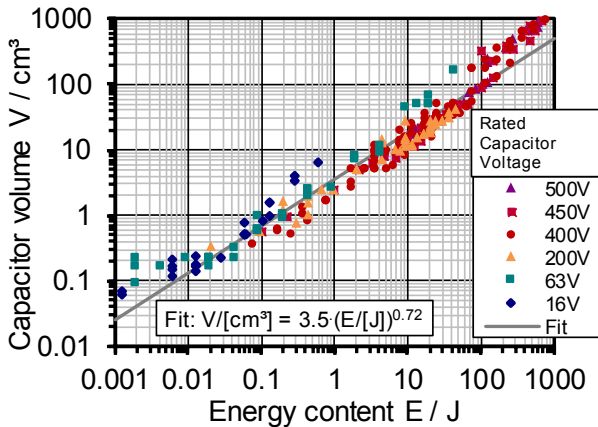


Figure 3: Volume size of electrolytic capacitors. Various electrolytic capacitors, data from [13].

This equation is used to illustrate in Figure 4 (orange trace), which E_{max} is necessary, if the required energy of 50 J is stored. The blue curve relates to the volume using the fit function in Figure 3.

The maximum voltage has no influence on the needed energy content of the capacitor and thus low influence on the capacitor size. The voltage can thus be freely selected from a capacitor point of view. Only the relative voltage difference, which can be considered as relative voltage ripple, determines the size. However, restrictions of the application have to be kept in mind: the grid inverter needs a minimum voltage to work correctly when directly connected to the grid (without a transformer) and the grid inverter cannot support too high voltage (due to semiconductors limits).

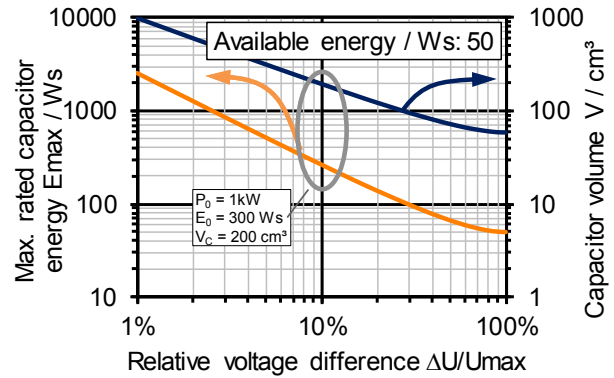


Figure 4: Needed capacitor energy and volume size to store 50 J.

Using the DC link capacitor the ripple should remain below 10%. To have 50 J available, this requires at least a rated energy content of 300 J, resulting in a capacitor volume of about 200 cm³ (e.g. 10 cm height, 5 cm diameter) to 400 cm³. Such a size could reasonably relate to a somewhat larger intermediate voltage capacitor of a 1 kW single phase converter.

4 POWER AND VOLTAGE FLUCTUATIONS

During daily operation, much smaller deviations from the desired operation point are expected than in a worst case. Therefore, this chapter shows the effect on the related components during daily operation, which gives an indication on their stress, rather than the worst case, which very seldom happens.

In a rotating generator, for small changes of power the rotational speed decreases while delivering a constant excess of power. Therefore, applying a virtual inertia, the required control power ΔP must be dependent on the time derivative of the frequency deviation Δf from the nominal frequency f_0 (50Hz):

(2)

$$\frac{\Delta P(t)}{P_0} = T_a \cdot \frac{d \Delta f(t)}{dt} \cdot f_0$$

P_0 is the nominal power of the system (in this case the power supply). ΔP is the power, which would be drawn from the grid by the power supply. If this value is positive, the converter takes less power, and thus “delivers” control power to the grid.

T_a is an inertia time constant, as commonly defined [14] [15] and toughed in lectures [16] [5]. In [15] $T_a = 24$ s is derived from a grid failure of the ENTSO-E grid (“Emslandvorfall”, 4.11.2006). This value is selected, because it relates to the real behaviour and a larger value of T_a gives the worst case in this paper. Figure 5 shows the measured frequency (orange) for one hour on 14.Aug. 2015. The data is measured by a team at the author’s university and is available on the author’s website [17]. Assuming an inertia time constant $T_a = 24$ s, the required power demand ΔP (blue) can be calculated from the time derivation of the frequency slope according to equation (2). The frequency is filtered with a running average using 3 averaged values to achieve reasonable results (red, overlaying with the unfiltered curve).

It is obvious that the required control power is only a very fraction in the range of less than $\pm 0.15\%$ of the rated power of the power supply. This shows that the hardware must not be changed, but is certainly able to provide the required control power during daily operation.

Usually, elcap sizes are selected by two criteria: Voltage ripple mitigation and lifetime due to current ripple. The current variation is well approximately proportional to the power variation. However, compared to the typical current ripple in an elcap, this amplitude of the current variations is more than an order of magnitude lower. In addition, the frequency of a less than a Hertz leads to the conclusion, that there is negligible additional impact on the elcap’s lifetime.

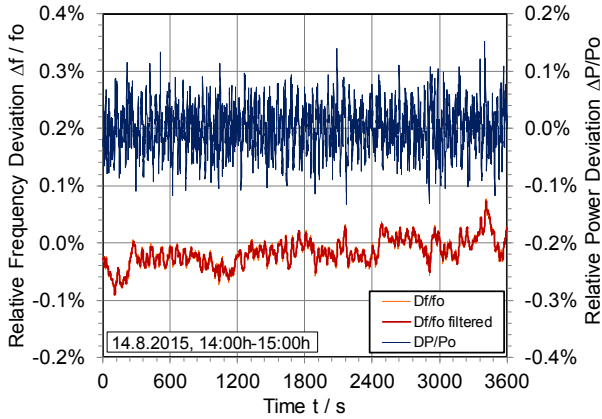


Figure 5: Measured frequency for one hour and related calculated control power $\Delta P/P_0$ with an inertia time constant $T_a = 24$ s.

The voltage change $\Delta U_C(t)$ on an intermediate voltage capacitor C can be calculated from the integral of the current $\Delta I(t)$. This charging current $\Delta I(t)$ results from the

control power $\Delta P(t)$. Assuming a fairly constant capacitor voltage of U_0 , results in:

$$\Delta U_C(t) = \frac{1}{C} \cdot \int \frac{\Delta P(t)}{U_0} dt \quad (3)$$

Considering equation (2), the integral cancels with the time derivative of the grid frequency. Expressing the capacity C by its nominal energy content E_0 results in:

$$\frac{\Delta U_C(t)}{U_0} = T_a \cdot \frac{1}{2} \cdot \frac{P_0}{E_0} \cdot \frac{\Delta f}{f_0} \quad (4)$$

This equation is used to calculate the voltage fluctuations on the intermediate voltage capacitor.

The required power is used to charge and de-charge a capacitor with typical maximum energy content of $E_0 = 300$ J, which relates to charging directly the DC-link capacitor (see above). From this the capacitor voltage and its fluctuation can be calculated. The calculated results are shown for one hour on 14. Aug. 2015 Figure 6 (blue curve).

The voltage variation during the investigated time remains between $\pm 3.6\%$ of the nominal voltage. This is a quite small value, which can be handled easily by power electronics. This shows that typical intermediate voltage elcaps can be used and no additional hardware is required to implement virtual inertia control in power supplies.

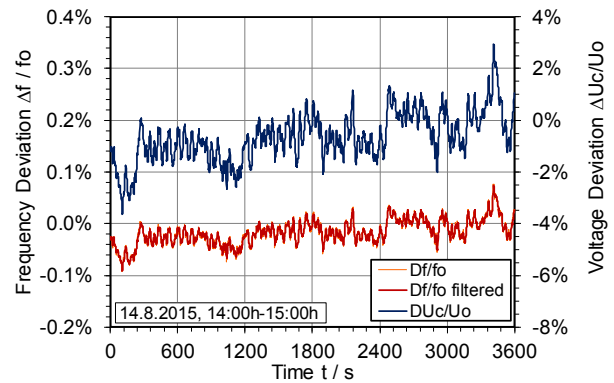


Figure 6: Measured frequency for one hour and related calculated voltage fluctuation on a capacitor with an energy content of 300 J.

5 CONTROL CONCEPT

Power supplies exceeding a certain nominal power are obliged to keep the power factor (including higher harmonics) the grid current within certain limits, e.g. lamp drivers exceeding 25 W (EN61000-3-2).

In most cases this is achieved with an active rectifier stage the power factor correction (PFC) circuit, which is

typically a step-up converter (see e.g. [18]). Figure 7 shows such a typical circuit. This power stage controls the power flow to the intermediate voltage capacitor: if the intermediate capacitor voltage decreases, there is too much power needed by the LED lamp and the converter increases the current, and thus the power from the grid. If the intermediate voltage is too high, the converter reduces the power. In general, the controller aims to keep the intermediate voltage constant at a given reference value. There are a number of issues associated with this control, but those details are not important for this particular approach.

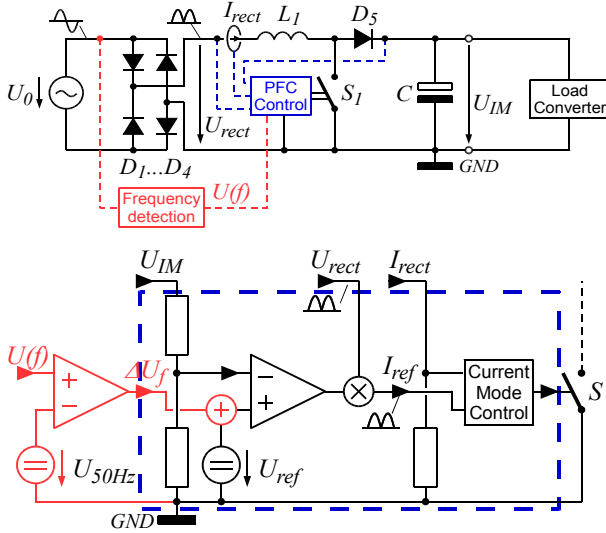


Figure 7: General control concept. Top: general block diagram of a PFC converter. Bottom: details of the control circuit. Red: Additions for the virtual inertia control.

The general idea is to hook up this existing control circuit with the virtual inertia control (red part). As derived in equation (4) the variation of the intermediate capacitor voltage should be proportional to the grid frequency variation. Therefore, the reference value for the intermediate voltage control gets an offset which is proportional to the grid frequency deviation provided by the f to V converter (“frequency detection”). If the grid frequency increases, the set value for the intermediate frequency is increased proportionally. Then, the controller sets the power such that the intermediate voltage follows the set value. According to equation (3) this leads inherently to the required dependence of the power on the derivative of the grid frequency as required for virtual inertia control (compare equation (2)). In addition, this kind of control makes sure that the intermediate voltage remains within necessary limits, because also the grid frequency must remain between given limits.

6 MEASUREMENTS

To prove the control concept of the virtual inertia, a lamp driver by Philips for a 35 W LED lamp, which includes a PFC stage, is used and modified. The type is the Philips Xitanium/Fortimo LED driver 110-3000TD/I (see Figure 8). Further details about the circuit and

measurements are described in [19]. Parts of these measurements are also used in [12] to demonstrate the concept presented there. The heart of the 46 W PFC consists of a controller chip TDA4863 by Infineon [20]. Figure 9 (top) shows the related part of the circuit diagram. Pin 1 of the chip is the input sensing the intermediate voltage, which is set down by the voltage divider consisting of R_5 to R_8 and $R_9||R_{10}$. Here, an additional signal, which offsets the sensed intermediate voltage, is added by resistor R_{21} . This voltage offset must be inversely proportional to the grid frequency deviation. If the intermediate voltage should increase, the sensed voltage must be lower such that it appears “correct” with increased intermediate voltage.

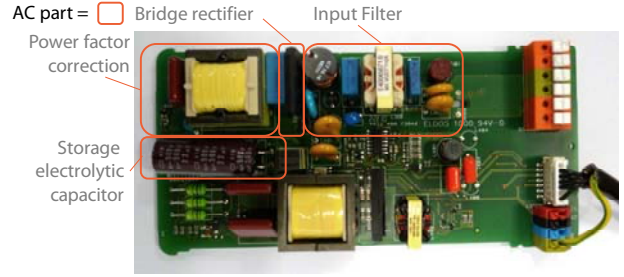


Figure 8: Printed circuit board of the modified LED driver.

As a proof, a voltage signal representing a frequency deviation is applied to this point. Figure 10 shows the measurement with a linearly increasing and decreasing signal (red) representing a linear decay and increase of the grid frequency. The orange curve shows the measurement of the intermediate voltage. It clearly follows the inverted control signal. The input power is shown in blue. It oscillates with 100 Hz. The dark blue curve shows the ideally expected power slope, which should be a square wave signal. The amplitudes of the voltage and power variations are exaggerated in this circuit compared to an operation in “real life” in order to demonstrate the functionality.

The measurement shows that indeed the input power nearly follows the square wave function. During the experiment no visual change of the LED brightness could be perceived showing that the second converter stage controlling the LED power worked well. This measurement proves that the controller of the input stage indeed behaves like needed according to equation (2) and provides the required function for the virtual inertia.

To demonstrate the reaction on the real grid frequency, a frequency to voltage converter is built as shown in Figure 9 (bottom). IC 1 (LM 2907) converts the grid frequency to a voltage. IC 2 subtracts to obtain a signal for the frequency deviation and IC 3 amplifies this signal, which is connected to the U_{sense} input of the controller. The complete circuit is tested on a synchronous generator providing a manually controlled varying grid frequency.

Figure 11 presents the measured results. The frequency is more or less linearly rising and decaying. The control voltage provided by the frequency to voltage

converter is shown inverted to compare it to the frequency. Furthermore, the intermediate voltage and the input power (averaged) are shown.

The red dashed line is provided to guide the eye. The control voltage follows the grid frequency roughly, but the shape is distorted and the signal is delayed. Especially the low-path filter (R8, C4) of IC1 contributes to this effect. Here a compromise had to be found to limit the ripple. The intermediate voltage follows the control voltage well. The input power variation can indeed be attributed to the derivative of the intermediate voltage as intended. However, due to the low path filter function, the power dependence on the frequency needs to be improved by optimizing the frequency detection circuit. If it could be integrated in the PFC controller chip a better performance can be anticipated.

7 CONCLUSIONS

Instantaneous power control of the power grid with electronic converters becomes necessary soon in Germany and Europe. It is shown that this requires additional power about 5 W with an energy of 50 J per event for each installed kW. The required storage size is in the order of magnitude as DC ripple cancellation capacitors in single phase converters. This means that existing hardware can be used and no significant additional storages like e.g. super capacitors or small batteries are needed. For an exemplary daily operation, the additional power ripple is in the order of 0.1% and an influence on the lifetime of the capacitors can be neglected. The voltage ripple of the intermediate voltage remains between $\pm 3.6\%$ of the nominal voltage and is thus easily covered by existing hardware. The related control can be easily extended by adding a voltage signal to the control voltage, which is

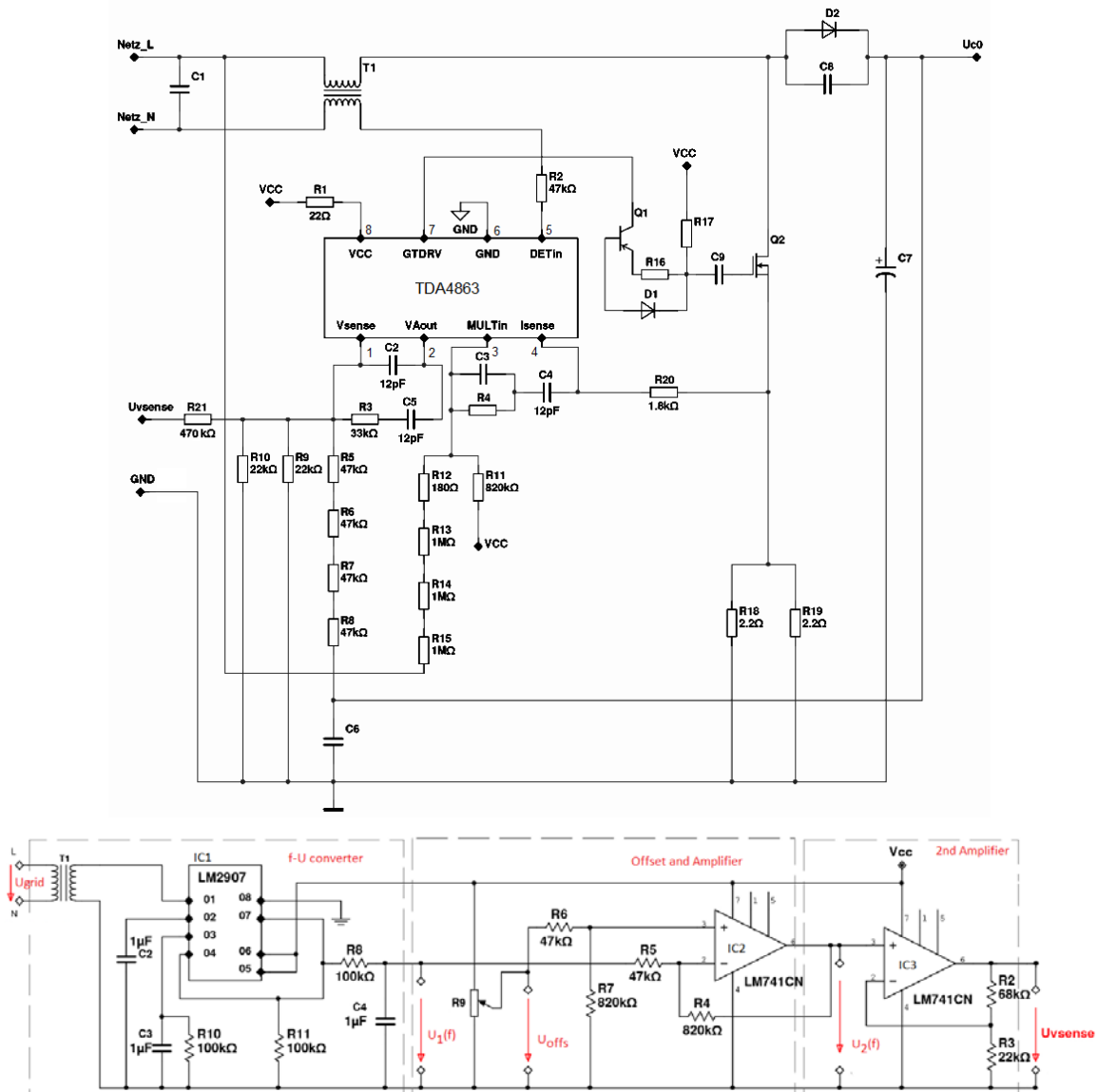


Figure 9: Circuit diagram of the modified PFC controller (top) and frequency to voltage converter(bottom)[19].

proportional to the frequency deviation. Then, the existing controller inherently sets the required additional power fluctuation required for the virtual inertia function. Concluding, no cost for additional hardware appear and only the control needs to be adapted.

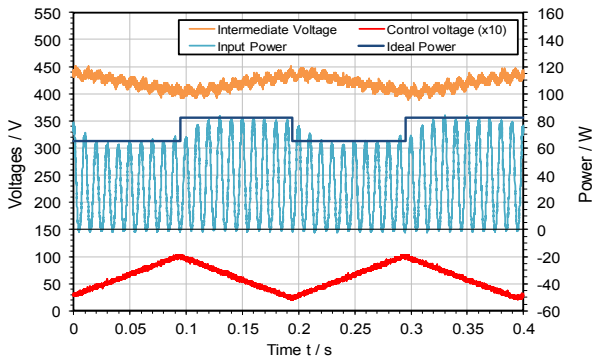


Figure 10: Measurements of the intermediate voltage (orange) and input power (blue) with a linearly increasing and decreasing control signal (red)

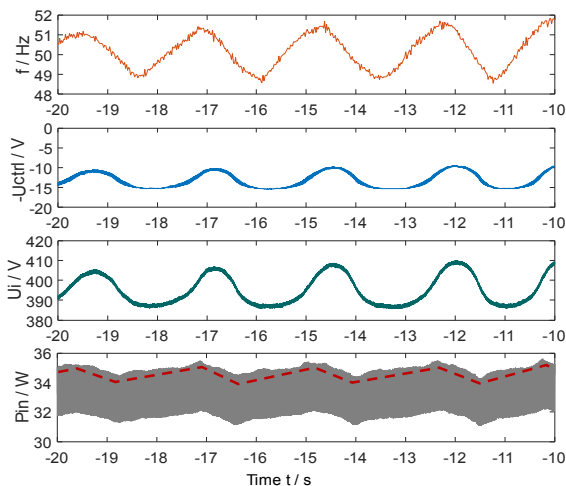


Figure 11: Measurement results with a grid voltage generated with a manually controlled synchronous generator.

ACKNOWLEDGMENT

The following persons contributed to this publication with parts of their student works: Daniel Wagner, Markus Korbmacher, Bente Muhr, Sonny Glesmann and Nora Kovacs. This work is related to the theme-based Research Scheme "Sustainable Lighting Technology: From Devices to Systems" supported by the Hong Kong Research Grants Council, Project reference T22-715/12-N.

REFERENCES

[1] Eberhard Waffenschmidt, "Dimensioning of decentralized photovoltaic storages with limited feed-in power and their impact on the distribution grid", *Energy Procedia* (2014), 31.Jan. 2014, pp. 88-97.

[2] Agora Energiewende, „Agormeter“, available online (12.June 2016), <https://www.agora-energiewende.de/de/themen-agothem-Produkt/produkt/76/Agormeter/>

[3] Bodo Giesler, Bruno Burger, "Erneuerbare Energien konkurrieren zunehmend mit Grundlastkraftwerken", *Proceedings of the 2. Oti-Konferenz „zukünftige Stromnetze für Erneuerbare Energien“*, 27.-28.Jan. 2015, p. 52-57.

[4] A.-C. Agricola, H. Seidl, S. Mischinger, et al., „dena-Studie Systemdienstleistungen 2030 - Sicherheit und Zuverlässigkeit einer Stromversorgung mit hohem Anteil erneuerbarer Energien“, Deutsche Energie-Agentur GmbH (dena), Energiesysteme und Energiedienstleistungen, Berlin, Germany, Feb. 2014.

[5] Albert Moser, "Elektrische Energieversorgungssysteme - Technische und wirtschaftliche Zusammenhänge", Skript zur Vorlesung "Elektrische Anlagen II", RWTH Aachen, Institut für Elektrische Anlagen und Energiewirtschaft, Forschungsgesellschaft Energie an der RWTH Aachen, 1. Auflage 2010, p. 342.

[6] Yong Chen, Ralf Hesse, Dirk Turschner, Hans-Peter Beck, "Improving the grid power quality using virtual synchronous machines", *Proceedings of the International Conference on Power Engineering, Energy and Electrical Drives (POWERENG 2011)*, 11.-13. May 2011, Malaga.

[7] Visscher, K.; de Haan, S.W.H.; Virtual synchronous machines for frequency stabilisation in future grids with a significant share of decentralised generation, *Proceedings of the CIRED SmartGrids conference*; June 2008; Germany

[8] Pedro Rodriguez, "Control of Grid-Interactive Power Converters: The Synchronous Power Controller", Presentation at ECPE-Workshop "Power Electronics in the Electrical Network", Kassel, Germany, 12. March 2013.

[9] Jonathan Brisebois, Noël Aubut, "Wind Farm Inertia Emulation to Fulfill Hydro-Québec's Specific Need", *Proceedings of the IEEE PES General Meeting - 978-1-4577-1002-5/11 Summer 2011*, July 24-28 2011. Detroit, Michigan, USA

[10] F. Gonzalez-Longatt, E. Chikuni, W. Stemmet, K. Folly, "Effects of the Synthetic Inertia from Wind Power on the Total System Inertia after a Frequency Disturbance", *IEEE PES PowerAfrica 2012 Conference and Exposition*, Johannesburg, South Africa, 9.-13.July 2012.

[11] "ENTSO-E Network Code for Requirements for Grid Connection Applicable to all Generators", ENTSO-E, 8 March 2013.

[12] E. Waffenschmidt, Ron S.Y. Hui, "Virtual inertia with PV inverters using DC-link capacitors", accepted for publication at ECCE/EPE 2016, Karlsruhe, Germany, 5.-9.Sep.2016.

[13] Conrad-Elektronik, Electrolytic Capacitors, Internet 6.7.2014: <http://www.conrad.de/ce/de/overview/0245812/Elektrolyt-Kondensatoren>.

[14] Martin Boxleitner, Günther Brauner, "Virtuelle Schwungmasse", 6. Internationale Energiewirtschaftstagung an der TU Wien (IEWT 2009), Wien, 2009.

[15] Philipp Strauß, "Einfluss des Frequenzverhaltens kleiner Generatoren und Lasten auf Stromnetze unter besonderer Berücksichtigung großer Netzstörungen", Dissertation (PhD Thesis) Universität Kassel, Technology & Science Publishers, Kassel, Germany, 2009, ISBN 978-3-00-029475-4

[16] B.R.Oswald, „Netzregelung“, Skript zur Vorlesung „Elektrische Energieversorgung 2“, korrigierte Fassung, Universität Hannover, Hannover, Germany, 2005.

[17] E. Waffenschmidt, „An der TH-Köln gemessene Netzfrequenz-Daten“, available online (12.June 2016), <http://www.100pro-erneuerbare.com/netze/messdaten/messdaten.htm#netzfrequenz>

[18] Miroslaw Mrozek, "Power Factor Correction Algorithm in AC-DC Converter", *Problemy Eksploatacji - Maintenance Problems*, 2-2013, p.129

[19] Nora Kovacs, "Momentanregelung mit Licht emittierenden Dioden (LED) Lampentreibern", Master Thesis at TH-Köln, 23. May 2016.

[20] "Boost Controller TDA4863 - Power Factor Controller IC for High Power Factor and Low THD", Infineon, Datasheet, Rev. 2, Feb. 2005.